European Journal of Operational Research 304 (2023) 139–149

Contents lists available at ScienceDirect

European Journal of Operational Research

journal homepage: www.elsevier.com/locate/ejor

OR in pandemics

Safe distancing in the time of COVID-19

Martina Fischetti[a], Matteo Fischetti[b,*], Jakob Stoustrup[c]

[a] Vattenfall BA Wind, Havneholmen 29, København 1561, Denmark
[b] Department of Information Engineering, University of Padua, via Gradenigo 6/A, Padova 35100, Italy
[c] Automation & Control, Department of Electronic Systems, Aalborg University, Fredrik Bajers Vej 7C, Aalborg 9220, Denmark

ARTICLE INFO

Article history:
Received 5 February 2021
Accepted 2 July 2021
Available online 10 July 2021

Keywords:
Combinatorial optimization
Social distancing
Mathematical optimization
Mixed integer linear programming
COVID-19

ABSTRACT

The spread of viruses such as SARS-CoV-2 brought new challenges to our society, including a stronger focus on safety across all businesses. Many countries have imposed a minimum social distance among people in order to ensure their safety. This brings new challenges to many customer-related businesses, such as restaurants, offices, theaters, etc., on how to locate their facilities (tables, seats etc.) under distancing constraints. We propose a parallel between this problem and that of locating wind turbines in an offshore area. The discovery of this parallel allows us to apply Mathematical Optimization algorithms originally designed for wind farms, to produce optimized facility layouts that minimize the overall risk of infection among customers. In this way we can investigate the structure of the safest layouts, with some surprising outcomes. A lesson learned is that, in the safest layouts, the facilities are not equally distanced (as it is typically believed) but tend to concentrate on the border of the available area—a policy that significantly reduces the overall risk of contagion.

1. Introduction

In this paper we study the optimal positioning of people in a common area, with the aim of minimizing the spread of viruses such as SARS-CoV-2.

The pandemic of 2020 has indeed put a new focus on safety across all our society. The re-opening of many countries after lockdown, in particular, puts new challenges for many businesses as they want to ensure safety of their customers and personnel, while still making a profit and offering their usual services. To ensure safety, many countries have introduced a minimum distance among people, the so-called *social distancing* constraint. This means that shared spaces (like offices, restaurants, theaters, etc.) are now facing a new challenge that concerns fitting customers while respecting social distancing restrictions and ensure safety. This leads to a kind of circle-packing optimization problem aimed at placing as many "facilities" (e.g., customers, tables, seats, etc.) as possible in a given area, while fulfilling the social distancing requirement. One example, that we will treat in more details in Section 5, can be a restaurant where we want to fit as many tables as possible in a given area.

Several recent studies consider optimal facility location subject to distancing constraints on settings such as airplanes and public transit.

Salari, Milne, Delcea, Kattan, & Cotfas (2020), address the problem of assigning passengers to seats on an airplane by fulfilling two types of social distancing constraints: passengers distance from each other, and passengers distance from the aisle of an airplane. A Mixed Integer Linear Programming (MILP) model is proposed and evaluated on an airbus A320 with twenty rows, single aisle and three seats on each side of the aisle.

Kudela (2020), formulates the problem of optimizing the usage of a given area under social distancing constraints, as a p-dispersion problem (Moon, 1984). The author uses the compact formulation for this latter problem recently proposed by Sayah & Irnich (2017), along with the decremental clustering method of Contardo (2020), and investigates the trade-off between the level of discretization and computational efforts on one side, and the value of the optimal solution on the other.

Pavlik, Ludden, Jacobson, & Sewell (2021), study the so-called Airplane Seating Assignment Problem to minimize transmission risks on airplanes, and provide two MILP models that can be effectively solved using a standard commercial solver.

Ugail et al. (2021), address the task of reconfiguring common physical environments subject to distancing constraints, and propose a methodology based on the solution of the well-known circle packing problem. The resulting optimal design tool is applied to a number of practical examples, including optimal seat assignment

* Corresponding author.
E-mail addresses: martina.fischetti@vattenfall.com (M. Fischetti), matteo.fischetti@unipd.it (M. Fischetti), jakob@es.aau.dk (J. Stoustrup).

https://doi.org/10.1016/j.ejor.2021.07.010
0377-2217/

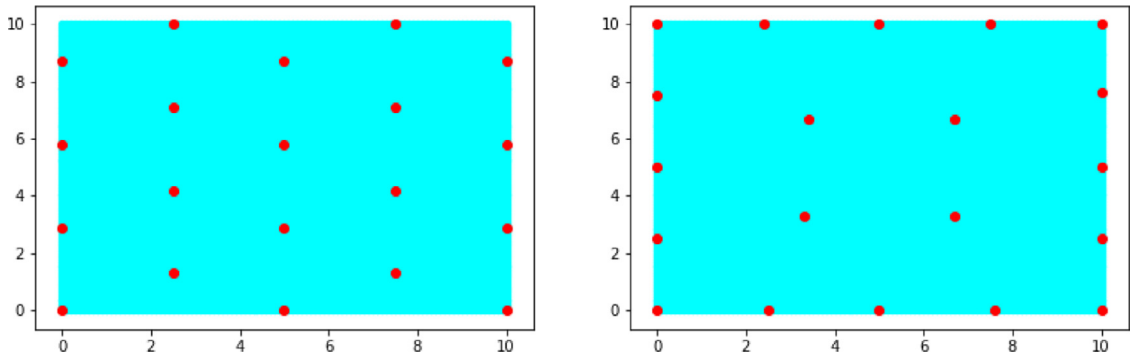

Fig. 1. Positioning 20 facilities within a square area with the objective of maximizing the minimum distance between facilities (subfigure on the left) or of minimizing the overall risk of infection (subfigure on the right). The difference between the two layouts is striking.

inside an airplane, optimal arrangement of chairs around tables of various forms, and optimal layout of the atrium area of a university campus building.

The paper by Moore, Carvalho, Davis, Abulhassan, & Megahed (2021), addresses seat assignment in Public Transit, and proposes a MILP model to assign passengers to seats based on the reported configuration of the vehicle and desired physical distancing requirement. A heuristic algorithm is also proposed, that deals with family groups for which the distance constraint can be relaxed. The two methods are evaluated through some illustrative scenarios (airplanes, school buses, and trains).

In our work we do not only look at the packing problem of locating as many facilities as possible in a given area, but we also focus on minimizing the overall virus spread. In this (more challenging) version of the problem the number of facilities is fixed and we want to find the safest layout that minimizes the overall risk of infection. One example can be a restaurant with a limited personnel capacity and a large room available for tables, where the strategy is to fit a predefined number of tables while maximizing the safety of the customers.

The intuition would tell us that, placing facilities at the maximum distance one from each other would ensure the safest layout. But is this really the case? Our experience on a different, yet similar, problem (the wind farm layout optimization problem; see, e.g., Fischetti, 2021; Fischetti & Monaci, 2014), allows us to verify the above intuition through computational experiments, thus bringing new light on the structure of the optimal solutions under different constraints and objectives.

Next, we introduce a simple example to better understand why considering the cumulative virus spread in the facility location problem is important, and how this impacts the final layout. Let us consider the allocation of 20 facilities on a square. These could be 20 tables to locate in a squared garden, for example. In Fig. 1 we report two optimal layouts, obtained by maximizing the minimum distance between facilities (subfigure on the left) or by minimizing the overall risk of infection (subfigure on the right); see the forthcoming Section 4 for more details about this experiment. The difference between the two layouts is striking: while the one of the left appears very regular, as expected, the one on the right looks strange at first glance, as it exploits the border of the available area to reduce the overall infection risk.

In this paper we provide a computational evidence that the safest layouts are often far from regular and depend on the geometrical shape of the available area. We show that positioning as many facilities as possible on the border of the available area tends to reduce virus spread, while the positions in the center of the area should be avoid as much as possible as they are surrounded in all directions by many other (potentially infectious) facilities.

The paper is organized as follows. In Section 2 we describe a related optimal layout problem arising in wind farm design, for which a Mathematical Optimization model is given in Section 3. Different functions modelling virus spread are introduced in Section 4 and evaluated on two simple cases. Some applications are illustrated in Section 5. Future directions of work are finally addressed in Section 6.

A preliminary version of the present paper (Fischetti, Fischetti, & Stoustrup, 2020a) circulated since May 2020 and was presented by the second author at the INFORMS 2020 meeting as the IFORS Distinguished Lecturer (November 12, 2020).

2. Optimal social distance and optimal wind farm layout

The professional expertise of the first author concerns the usage of optimization in the design phase of wind farms. Among other topics, she worked on the offshore wind farm layout optimization problem, which consists in deciding where to place turbines in a given area in order to maximize production while reducing costs (Fischetti, 2019; 2021; Fischetti & Fraccaro, 2019; Fischetti & Monaci, 2016; Fischetti & Pisinger, 2019). As we will see, this problem has many similarities with the facility location problem at hand. Let us introduce the reader to the wind farm layout optimization problem first, so that the similarities with the problem at hand will become clear.

The offshore wind energy business in Europe is based on an auction system where a country puts a well-defined offshore area on tender, and different companies bid on the the rights to construct the wind farm in that area. The company that can provide energy at the lower cost will get the right to construct and operate the new offshore wind farm. Therefore, each company wants to design the new wind farm minimizing costs and increasing profitability. This task typically involves optimizing the placement of turbines within the given area. A key aspect in the optimization is to take wake effects into account. The wake effect is the interference phenomenon for which, if two turbines are located close to one another, the upwind turbine creates a shadow on the downstream one; see, e.g., Odgaard & Stoustrup (2013). This is of great importance in the design of the layout since it results in a loss of power production for the turbines downstream, that are also subject to a strong (hence damaging) turbulence; see Fig. 2 for an illustration.

Given a certain wind scenario, defined by the wind intensity and direction, the wake effect can be simply modelled as a cone, centered in the upwind turbine, that fades away with distance (Jensen, 1983). Nevertheless, when the wind farm layout problem is solved during the design phase, one needs to consider the full variability of the wind. As a matter of fact, considering only one

Fig. 2. Wake effect on a real wind farm (Horns Rev 1): regular layouts like the one in the picture can be very inefficient for certain specific wind scenarios, resulting into a greatly reduced energy production for the whole wind farm. [Source: Vattenfall].

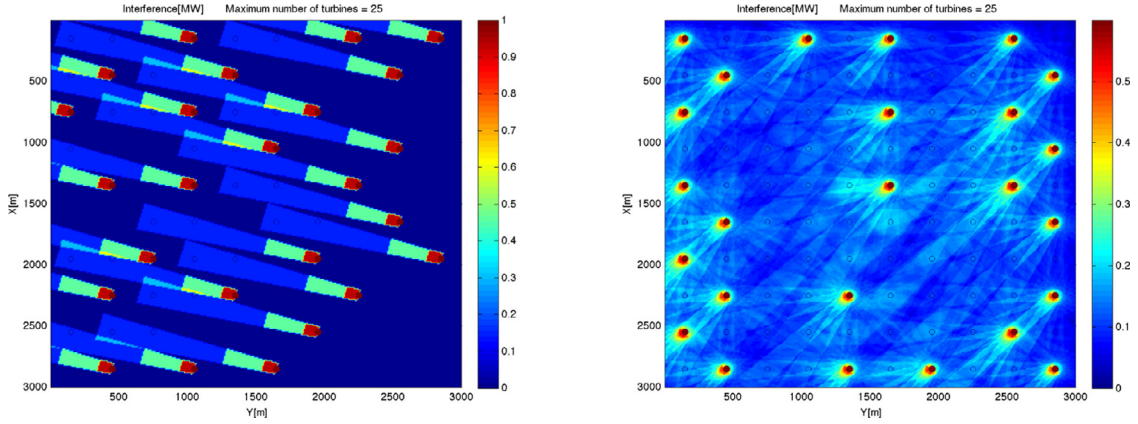

Fig. 3. The interference among turbines can be visualized as a cone when only one wind scenario is considered (left plot). In the design of an offshore wind farm, however, the full variability of the wind needs to be considered, as visualized in the right-hand-side plot. [Source: Fischetti (2018)].

wind scenario would create a layout which is optimal for that specific wind condition, but potentially highly suboptimal when the wind changes intensity and/or direction. In Fischetti & Monaci (2016), a method to consider the full variability of the wind when optimizing the layout, is proposed. Intuitively, this method lets the optimizer consider a weighed intersection of the interference cones for all possible wind scenarios, where more likely scenarios have a higher weight in the combination. Visually, this means that the interference becomes a star of cones around the turbine. In practical applications with thousands of possible wind scenarios, this star is so dense that it looks like a continuous interference shade around the turbine, with more intense values in the main wind directions; see Fig. 3 for an illustration.

In practical applications, a minimum and/or maximum number of turbines to be located in the area can be imposed, together with a minimum distance among turbines (to avoid the blades clash, and also for turbulence considerations). There can be obstacles within the offshore area (such as natural reserves, preexisting infrastructures, bad seabed areas etc.), which are areas where the turbines cannot be located. The wind farm layout optimization problem therefore consists in locating a given number of turbines (or as many as profitable) in a given area, ensuring a minimum distance among turbines and minimizing the interference among them.

What about our problem about social distancing in a public place such as a restaurant? It also consists of locating a given number of facilities (tables or customers) in a given area, ensuring a minimum distance among them (legal or recommended social distance) and minimizing the potential virus spread among facilities.

In the wind farm layout problem, the interference is a well-studied function that represents the loss of power due to wake effect. In the social distancing problem, instead, the interference is a function that represents the spread of the virus. Both interference interpretations depend on the distance—the further the lower.

Our experience on the wind farm layout problem shows that optimal layouts tend to use the borders of the available area, where the turbines create less interference with other turbines. It also shows that traditional manual layouts where turbines are placed on a regular grid, are highly sub-optimal as significantly higher production can be achieved by a smarter placement of turbines. The resolution of the problem in practical applications is far from trivial, and state-of-the-art Mathematical Optimization techniques have proved to make a huge impact in the practical resolution of the problem (Fischetti, Kristoffersen, Hjort, Monaci, & Pisinger, 2020b).

3. Optimization model (for wind farms)

In Fischetti & Monaci (2016), the first author proposed a MILP model for the wind farm layout problem. The overall area available is sampled to define a discrete set V of possible positions, and a binary variable x_i is defined for each $i \in V$, taking value 1 if and only if a turbine is built at position $i \in V$.

The optimizer considers:

a) a minimum and maximum number of turbines that can be built;
b) a minimum separation distance between any pair of turbines, to ensure that the blades do not physically clash;

c) the interference among installed turbines (wake effect).

Let

- I_{ij} be the interference (loss of power) experienced by position j when a turbine is installed at position i, with $I_{jj} = 0$ for all $j \in V$; Jensen's model (Jensen, 1983) can be used to compute such an interference;
- P_i be the power that a turbine would produce if built (alone) at position i;
- $N_{\min}$ and $N_{\max}$ be the minimum and maximum number of turbines that can be built, respectively;
- d_{ij} be the distance between positions i and j;
- $D_{\min}$ be the minimum distance required between two turbines.

In addition, let $G_I = (V, E_I)$ denote an "incompatibility" undirected graph with

$$E_I = \{[i, j] : i, j \in V,\ d_{ij} < D_{\min},\ i < j\}.$$

A natural quadratic objective function (to be maximized) for our problem reads:

$$\sum_{i \in V} P_i x_i - \sum_{i \in V} \sum_{j \in V} I_{ij} x_i x_j \tag{1}$$

and can be restated as

$$\sum_{i \in V} (P_i x_i - w_i) \tag{2}$$

where the continuous variable w_i is defined as

$$w_i = \Big(\sum_{j \in V} I_{ij} x_j\Big) x_i = \begin{cases} \sum_{j \in V} I_{ij} x_j & \text{if } x_i = 1; \\ 0 & \text{if } x_i = 0 \end{cases}$$

and denotes the total interference caused by a turbine built in position i. The MILP model then reads:

$$\max z = \textstyle\sum_{i \in V} (P_i x_i - w_i) \tag{3}$$

$$\text{s.t. } N_{\min} \le \textstyle\sum_{i \in V} x_i \le N_{\max} \tag{4}$$

$$x_i + x_j \le 1,\ [i, j] \in E_I \tag{5}$$

$$\textstyle\sum_{j \in V} I_{ij} x_j \le w_i + M_i (1 - x_i),\ i \in V \tag{6}$$

$$x_i \in \{0, 1\},\ i \in V \tag{7}$$

$$w_i \ge 0,\ i \in V. \tag{8}$$

The objective function (3) maximizes the total power production by taking interference losses into account. Constraints (4) impose a minimum and a maximum number of turbines that can be constructed in the area. If $N_{\min} = N_{\max}$, then we are actually imposing a fixed number of turbines, otherwise the optimizer can define the best number of turbines (within $N_{\min}$ and $N_{\max}$) to be located. Constraints (5) ensure the minimum distance between turbines. Constraints (6) force the correct value for variables w_i; here, a big-M term $M_i \gg 0$ is used to deactivate the constraint in case $x_i = 0$, namely

$$M_i = \sum_{j \in V : [i,j] \notin E_I} I_{ij}.$$

Finally, constraints (7) and (8) define our binary and continuous variables, respectively. As shown in details in Fischetti & Monaci (2016), using a single index variable w_i allows this model to solve larger instances compared with equivalent two-index models in the literature (e.g., Archer, Nates, Donovan, & Waterer, 2011; Fagerfjall, 2010). Another strength of this formulation is the ability of easily dealing with multiple wind scenarios; the reader is again referred to Fischetti & Monaci (2016), for further details.

Based on the above model, a sound matheuristic (Fischetti & Fischetti, 2018) solution approach has been developed in Fischetti & Monaci (2016).

4. Modelling virus spreading

Wake effects among turbines have been largely studied in the wind energy literature, and well-established interference models exist in the literature (Jensen, 1983). Recent literature related to the transmission of airborne SARS-CoV-2 infections includes, among others, Morawska et al. (2020); Noakes, Beggs, Sleigh, & Kerr (2006); Prather et al. (2020); Samet et al. (2021); Tang et al. (2021); Zhao, Cheng, Liu, & Sun (2020) and references there-in.

Mittal, Meneveau, & Wu (2020), estimate the risk of airborne transmission of a respiratory infection such as COVID-19 through a simplified mathematical model based on basic concepts from fluid dynamics. The model is intended to provide a common basis for scientific inquiry across disciplinary boundaries and allows one to quantify the reduction in the transmission risk associated with increased physical distance between the infected person and a "susceptible" individual.

Jones et al. (2021), give a mathematical model to estimate the SARS-CoV-2 infection risk in a well-mixed indoor space, as a function of space volume, viral emission rate, exposure time, occupant respiratory activity, and room ventilation.

Next, we analyse alternative functions that can be used to define the interference matrix (I_{ij}) measuring the infection risk between an infected person in position i and a susceptible individual in position j. We aim at evaluating the impact of alternative interference definitions in providing optimized layouts where the facilities are scattered as much as possible in the available area even when $D_{\min} = 0$, i.e., even without imposing explicitly a minimum distance among facilities.

Note that, for the purpose of the optimization, one can omit a constant factor in the definition of the interference, meaning that the optimal layout does not depend on the actual value of some important epidemiological parameters such as virus emission rate, exposure period etc.—which are in fact only needed to quantify the actual *value* of the infection risk.

It is important to stress here that we do not address the delicate issue of deciding which deterministic functional form of the interference is best to describe the transmission of the virus—a topic to be addressed by the vast scientific community of epidemiologists and virologists. Indeed, the interference function is just an input data for our model, whose definition is delegated to the decision maker.

Let d_{ij} represent the Euclidean distance (in meters) between positions $i, j \in V$, and let $d_{\max}$ be the maximum such distance. We consider the following alternative definitions for the interference I_{ij} that a facility located at position i causes to a customer in position j at a distance $d_{ij} \ge 10^{-4}$; by convention, $I_{ij} = 0$ whenever $d_{ij} < 10^{-4}$, which implies $I_{ii} = 0$ for all $i \in V$:

$$I_{ij} \propto d_{max} - d_{ij} \tag{9}$$

$$I_{ij} \propto e^{-d_{ij}^2/2} \tag{10}$$

$$I_{ij} \propto 1/d_{ij} \tag{11}$$

$$I_{ij} \propto 1/d_{ij}^{1.5} \tag{12}$$

$$I_{ij} \propto 1/d_{ij}^3. \tag{13}$$

Definition (9) considers an infection risk inversely proportional to the distance. At first glance, this would seem a reasonable assumption, but it turns out to be a very bad choice: even when positioning just 3 facilities on a line segment, an optimal solution will position two facilities and the endpoints of the segment, while the third one can freely be located at any other point of the segment without affecting the solution value—while we would expect the optimal solution be unique and place the third facility on the middle point of the segment.

Definition (10) assumes the infection risk can be modeled as a Gaussian function with variance $\sigma^2 = 1$. This can be a realistic assumption to model the trajectory of large droplets, which are expected to decay rapidly and fall down within 1–2 m or so.

Definitions (11) and (12) are taken from Mittal et al. (2020) (Sect. VII-B), where the protection due to physical distancing is studied in different outdoor wind scenarios. Definition (11) corresponds to, e.g., "a sedentary individual breathing at a low exhalation rate in still wind conditions", while definition (12) corresponds to, e.g., "persons breathing normally with an expiratory velocity of $\approx$ 1 m/s on a windy day with wind velocities of 10 miles/h".

Definition (13) is based on the work of Jones et al. (2021), and assumes a steady-state condition where virus aerosol is spread uniformly. Indeed, in the 3-dimensional space a sphere of ray d_{ij} centered at position i (where the virus aerosol is emitted) has a volume proportional to d_{ij}^3. Thus, assuming a uniform virus distribution within the sphere, the virus concentration at position j is proportional to $1/d_{ij}^3$.

When I_{ij} has been defined, we assume that the "total virus exposure" (i.e., the infection risk) experienced by a customer sitting in position j is computed as

$$\sum_{i \in V, i \neq j} I_{ij} x_i,$$

where $x_i = 1$ if a potential source of virus (e.g., a potentially infected customer) is present at position i, and $x_i = 0$ otherwise.

As already discussed, we are interested in defining the interference matrix (I_{ij}) in a way that favors the spread of facilities on the available area, even without imposing a minimum distance as a constraint. In the next subsections, we consider regular 1- and 2-dimensional areas and compare the optimised layouts resulting from the alternative interference definitions. In those experiments, we fix the number k of facilities to be located (by setting $N_{\min} = N_{\max} = k$), we define $P_i = 0$ for all $i \in V$ (no power production), and we do not require any minimum distance among facilities ($D_{\min} = 0$). In this way, we only evaluate the effect of the alternative interference-matrix definitions in producing scattered layouts.

4.1. Positioning facilities on a line

In Fig. 4 we consider the problem of positioning 10 facilities on a line segment, using the alternative interference definitions (9) to (13). As expected, the two endpoints of the segment are selected in all cases—using the border of the available area turns out to be a successful policy in wind farm design as well. The layout in the top subfigure (definition (9)) is completely unsatisfactory in terms of social distances, as the selected points define two clusters of five points each, located beside the line endpoints. The second layout based on the Gaussian function (10) is more regular, but still uses two pairs of almost-overlapping positions beside the line endpoints. The remaining layouts are obtained with (11) to (13) and allow for a satisfactory distancing among facilities.

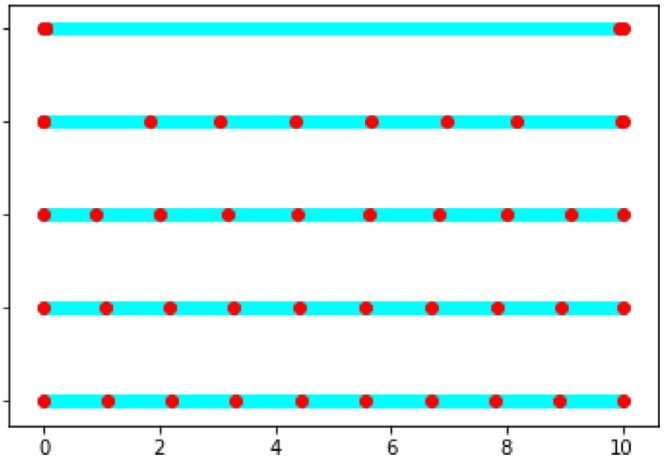

Fig. 4. Positioning 10 facilities on a line using interference definitions (9) to (13) (from top to bottom).

4.2. Positioning facilities within a square

In Fig. 5 we consider the problem of positioning 20 facilities within a 10m x 10m square. As expected, the border points are very attractive, and the four edges contain most of the built facilities. As in the 1-dimensional case, definition (9) produces clusters of facilities on the four vertices of the square (top-left subfigure). Using the Gaussian function (10) produces the more satisfactory layout of the top-right subfigure, while the bottom-left subfigure refers to (11). The most satisfactory layouts are obtained using definition (12) (bottom-right subfigure) and (13) (not reported as identical to the one in the bottom-right subfigure).

The structure of the optimal layouts reported in the two bottom plots of Fig. 6 is quite interesting and deserves some additional comments. First of all, the two layouts look quite different, confirming that the definition of the virus-spread function plays an important role here. Even more importantly, both solutions exhibit a certain degree of symmetry, but the facilities are not allocated on a regular grid. In particular, the distance among the allocated facilities is not uniform—the facilities tend to cluster on the four edges of the square, a policy that allows for a larger distance among those allocated in the central area where virus concentration tends to be higher.

As expected, the optimal layouts with interference definitions (10) to (13) exhibit a significant distancing among the facilities—although this is not imposed through an explicit constraint. In particular, the minimum distance among facilities when using interference definitions (10)–(13) is equal to 2.57 m, 1.80 m, 2.40 m and 2.50 m, respectively.

Fig. 6 plots the total interference $\sum_{i \in V} I_{ij} x_i$ perceived by each point $j \in V$, by using alternative interference definitions. In the virus-spread context, this is proportional to the probability of infection that depends on the location of all the built facilities. The top-left subfigure confirms once again that definition (9) is not adequate to represent virus spread, as the probability of infection is almost uniform in the square—the total interference ranges from about 140 in the center, and about 100 in the four corners where the facilities are clustered.

It is worth observing that the optimal layouts produced by the two alternative definitions (12) and (13) are almost indistinguishable, although they would correspond, in principle, to two different virus-spread scenarios. According to our experience, having an interference $I_{ij} \propto 1/d_{ij}^k$ with $k \in \{1.5, 2, 3\}$ produces essentially the same optimal layout, meaning that the latter is very robust with respect to this type of changes of the interference function.

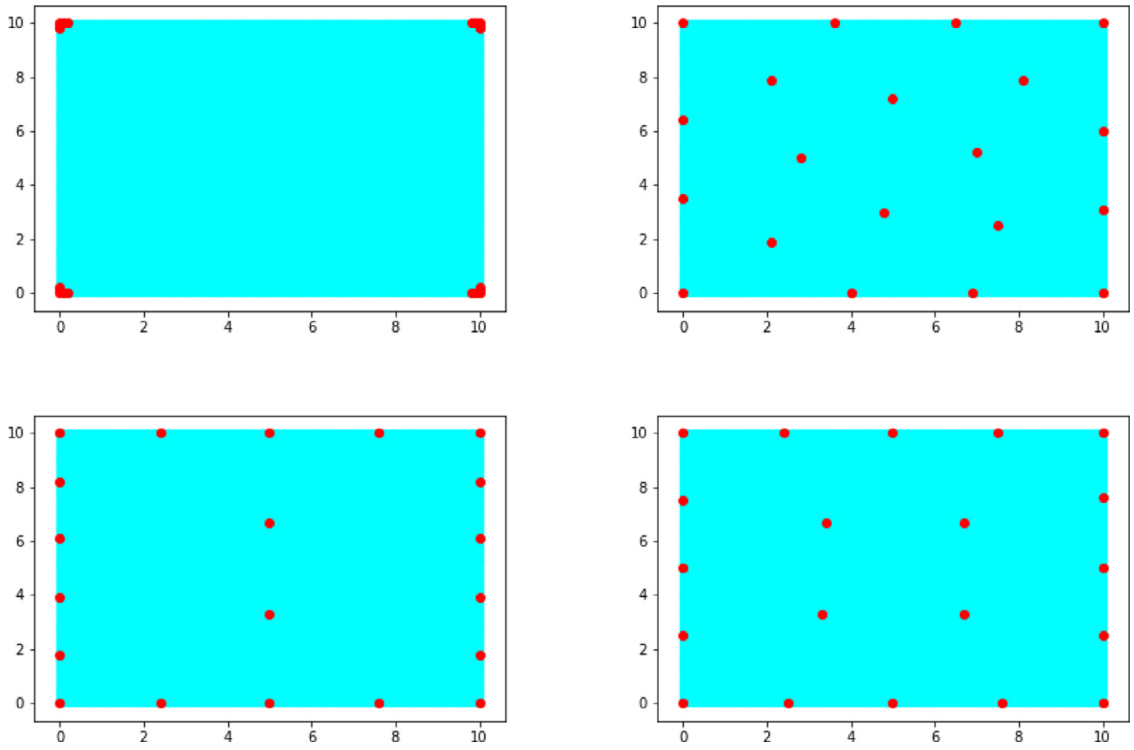

Fig. 5. Positioning 20 facilities within a square area using definitions (9) (top-left) to (12) (bottom-right). The plot using definition (13) is almost identical to the one reported in the bottom-right subfigure; hence it is omitted.

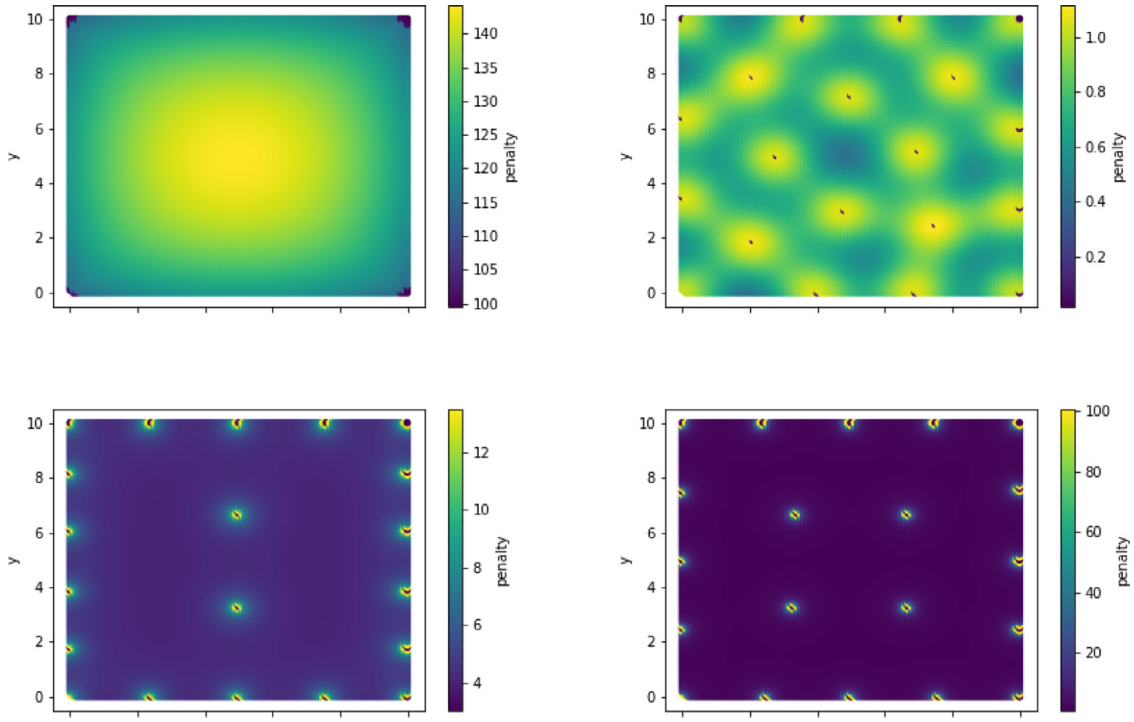

Fig. 6. Penalty measuring the infection level (i.e., the total interference) using the interference definitions (9) (top-left subfigure) to (12) (bottom-right subfigure). Penalty scales are different in each subfigure. The plot using definition (13) is almost identical to the one reported in the bottom-right subfigure; hence it is omitted.

Fig. 7. Example of optimization of table placement for the outside serving area of a brewpub in Denmark. The available area for placing tables is highlighted in the second plot.

5. Applications

We next address some practical examples of optimized facility layout under social distancing constraints.

5.1. Restaurants

Let us suppose we own a restaurant which has a certain space to place customer tables (an indoor room, or a given outdoor space). We have to ensure a minimum distance among tables, as imposed by the local government regulations, and at the same time we want to fit as many tables as possible—even one more table can make a difference in the final income for the day. Also, among the feasible layouts we would like to choose one that minimizes the infection probability of the customers, measured through a suitable "virus spread" function—we used definition (13) in our experiments. Most restaurants are solving this optimization challenge manually, often by placing tables aligned in rows and at a regular distance. As we will see, optimized solutions for this problem are not as regular as the manual ones—positioning tables in a less-regular but smarter way can satisfy more customers and also reduce virus spread.

We next consider the real case of a brewpub in Denmark (Brus, Copenhagen) with an available outdoor area where tables can be placed. Using online satellite views (first plot of Fig. 7) we identified the available area for tables (red area in the second plot of Fig. 7). Note that the presence of a tree does not allow to place tables in the middle part of the area, which was therefore excluded from the set of available positions.

5.1.1. Fitting more tables under social distancing rules

The first problem we would like to solve is to place as many tables as possible in the available area, while of course complying with the minimum distance among tables imposed by country's regulations. In our model, this is easily obtained by setting $N_{\min} = 0$, $N_{\max} = +\infty$, $D_{\min}$ to the required value (e.g., 3 m center-to-center), and all P_i's to a large positive value (10^3 in our experiments).

A naïve way to manually solve this problem is to locate tables on a regular grid, starting from a corner of the available area and locating each new table at the given minimum distance. This manual layout locates 30 tables (red dots in the first plot of Fig. 8), while our optimization method could locate 36 tables (red dots in the second plot of Fig. 8). Having 6 more tables increases by 20% the capacity for customers and can make a significant difference in terms of daily profits of the brewpub—without impacting the compliance to the local social distancing rules (here assumed to be 3 m) and the safety of the customers.

It is clear from this test that the optimal placement of tables is not straightforward, and that the usage of optimization methods can significantly increase the capacity of a restaurant to fit customers, and thus its daily revenue.

5.1.2. Fitting a given number of tables while minimizing virus spread

Another variant of the problem consists in fitting a fixed number of tables in the area, while maximizing the safety of the customers. For this test, we fit 30 tables as in the manual solutions, but in a safer way. This is simply obtained in our model by setting $N_{\min} = N_{\max} = 30$. We use the virus-spread functions (13) to measure the risk of infection among tables. The resulting layout is shown in Fig. 9. As expected, many tables are located on the border of the area. Note that the optimal layout is quite irregular, due to the need of coping both with the irregularity of the available area and with the complex interference pattern among tables.

5.1.3. Total risk of infection vs number of allocated tables

In Fig. 10 we plot the Pareto-optimal frontier of the bi-objective version of the problem aimed at maximizing the number of allocated tables while minimizing the total risk of infection. A minimum distance of 3 m has been imposed as in the previous examples. We use the virus-spread functions (13) to measure the risk of infection among tables, normalized to 1 for the case with 36 tables. As expected, the curve is nonlinear, with a slope increasing when the number of tables approaches its maximum value of 36. Indeed, the total risk of infection remains quite low (less than 20% with respect to its maximum level) up to 22 tables, then quickly increases to about 60% with 30 tables, and goes to 80% with 33 tables.

5.2. Beach umbrellas

Another possible application of our optimization method is the optimal placement of umbrellas on a beach. Many seaside activities are indeed challenged by the COVID-19 restrictions, and owners of seaside areas can face difficulties in secure their income while ensuring safety. In countries like Italy, many beach areas are managed by private owners, who rent beach facilities (such as umbrellas,

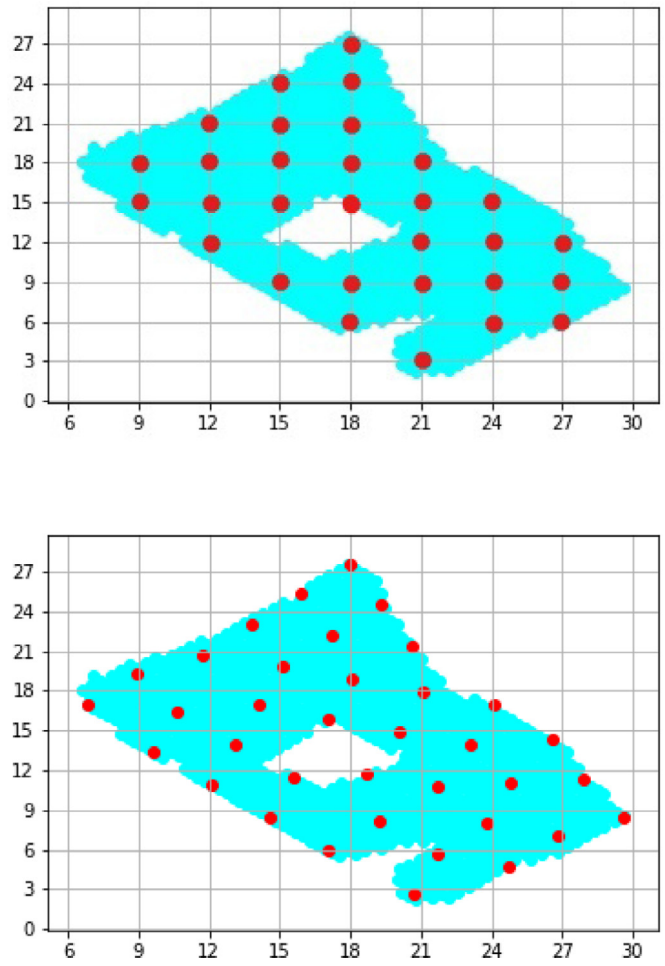

Fig. 8. Example of optimization of table placement for the outside area of "Brus" brewpub in Denmark. Tables are placed following a manual approach (based on a super-imposed 3 m × 3 m regular grid) in the first plot. The second plot shows the optimized placement of tables at a minimum of 3m distance, using an optimization tool: 6 more tables can be located.

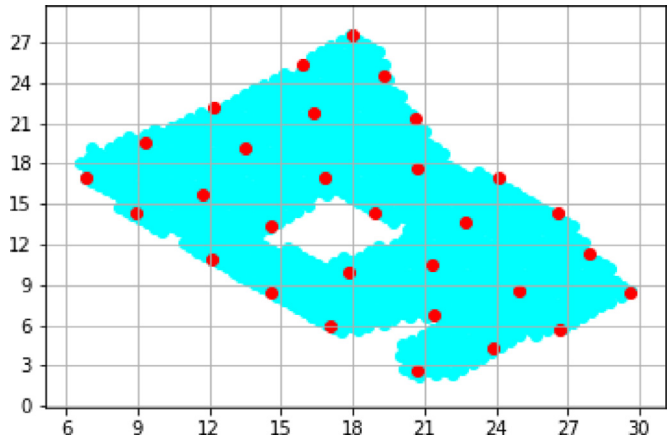

Fig. 9. Minimizing virus spread for a fixed number of facilities smaller than the maximum capacity.

sunbeds, chairs, etc.) to customers. Due to COVID-19, social distance limitations also apply in defining the exact position of the umbrellas on the beach. Using optimization methods can have a big impact also in this case, allowing one to fit more customers while not compromising on their safety. For example, considered the real case of the beach "Bagni Alberoni" located in Venice, Italy. The first plot of Fig. 11 shows the actual layout designed by the beach owner to cope with the required 4 m minimum distance among umbrellas. This solution locates 203 umbrellas in the available area. We gave the same area (blue in the second plot of Figure) on input to our optimizer, together with the minimum distance of 4 m. The interference definition (13) was considered. Our optimizer was able to fit 211 umbrellas–having 8 more umbrellas to rent out over the summer season, can make a significant economic impact for local business. On the other hand, the optimal layout appears quite irregular, so it might appear "quite messy" at first glance.

5.3. Family-group seat selection in a theater

In the previous sections we looked at the allocation of facilities, such as tables or umbrellas. Our model can be extended to

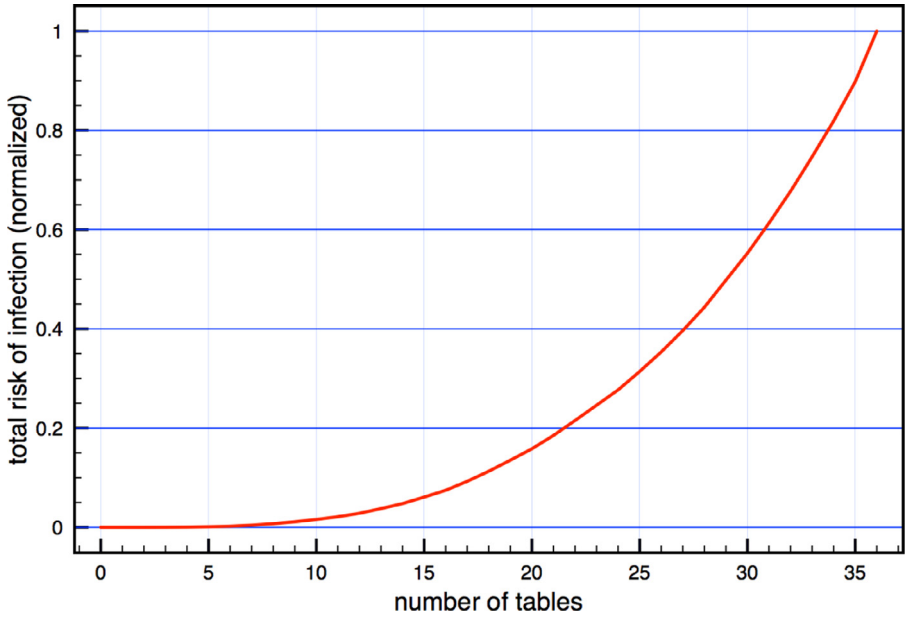

Fig. 10. Trade-off between number of allocated tables and total risk of infection..

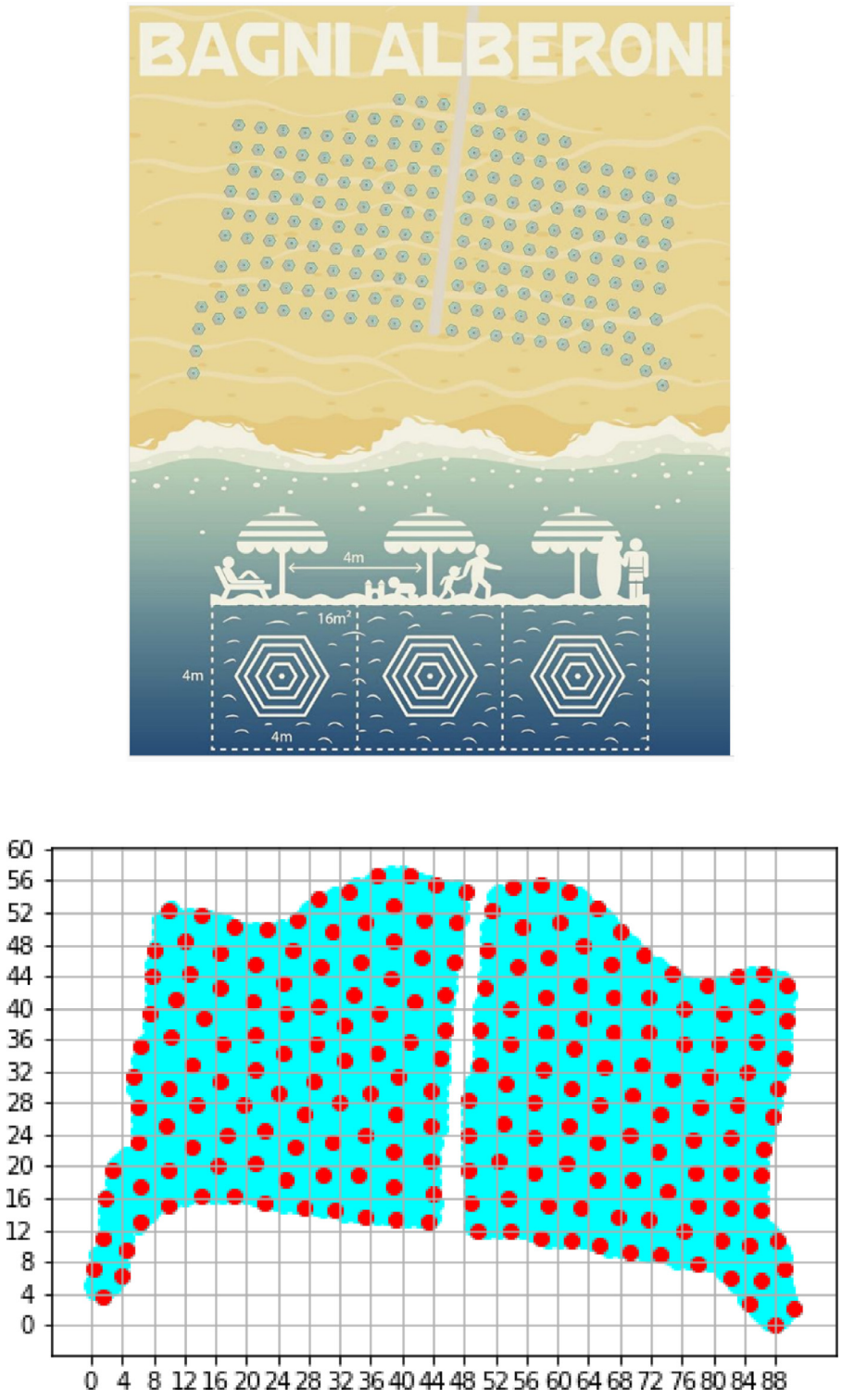

Fig. 11. Example of a real case—the Venice beach "Bagni Alberoni". Beach umbrellas must ensure a minimum distance of 4 m (center-to-center). The manual solution actually implemented (top) allocates 203 beach umbrellas, while the optimized one (bottom) is able to fit 211 beach umbrellas using a less-regular pattern.

optimize seat selection, for example in theaters or transport systems such as airplanes. The two versions of the problem are similar yet slightly different: the seat selection problem still must deal with minimizing the spread of viruses and fulfilling social distance limitations, but it also needs to consider "family groups" which are allocated in consecutive seats without fulfilling the minimum-distance requirement. In other words, compared to the problem statement so far, we now allow family members to seat close to each other, while the usual social distances regulations apply among different family groups. Thus, given a set of available seats, we want to optimize seat allocation by considering the presence of family groups and the imposed feasibility rules.

Fig. 12 shows the real case of the "Det Andre Teatret" (DAT) amphitheater in Oslo. The plot on the left shows the overall seating area available, while the plot on the right shows a seat allocation that considers family groups of different sizes. For the amphithe-

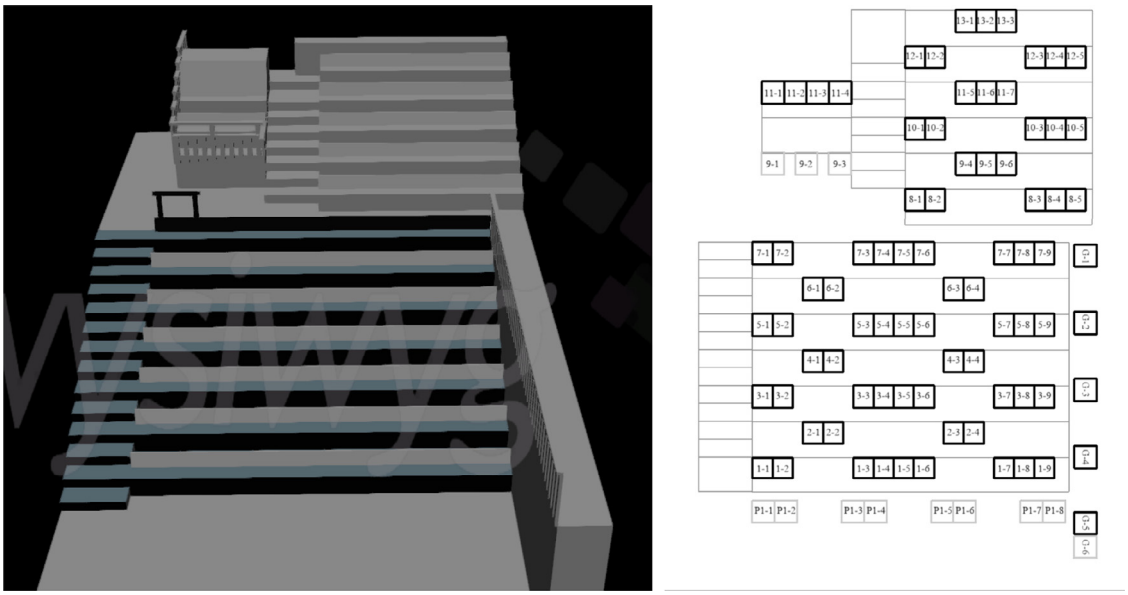

Fig. 12. Seat allocation of family groups at Oslo's "Det Andre Teatret" (DAT) amphitheater [figure source: private communication].

ater, the Norwegian guidelines from the government, at the time of writing, are as follows: (1) one empty seat in between people who belong to different groups and sitting on the same row; (2) a person from one group cannot sit directly behind a person from another group.

The family-group seat selection problem can easily handled by our model by listing all the possible consecutive-seat *configurations* involving groups of $1, \ldots, k$ family members, where k is the maximum family size allowed. E.g., a possible configuration for a group of 3 family members can be the consecutive-seat triple (7–7, 7–8, 7–9) of Fig. 12 (right).

Let V denote the set of all possible configurations. Thus, in model (3)–(8) the binary variables x_i's are associated with configurations, and the incompatibility (and interference) between configuration pairs $i, j \in V$ is easily computed according to the imposed regulations. Finally, the cardinality constraints (4) are replaced by

$$N^t_{\min} \le \sum_{i \in V^t} x_i \le N^t_{\max}, \qquad t = 1, \ldots, k \tag{14}$$

where V^t is the set of the configurations involving a group of t members, and $N^t_{\min}$ and $N^t_{\max}$ are the pre-specified minimum and maximum number of groups with t members that need to be allocated, respectively (this latter information being provided, on input, by the theater).

For example, the DAT case of Fig. 12 produced a model with 506 configurations and 11,726 forbidden configuration pairs. Interference I_{ij} between each configuration pair (i, j) has been computed through the virus-spread function (13), where the 2D coordinates of middle seat of the configurations are considered when computing the distance d_{ij}.

6. Conclusions and future work

In this paper we have studied the problem of locating facilities (tables, seats, etc.) in a given area, subject to social distancing constraints as those arising in the time of COVID-19. Our goal is to provide the decision maker with a sound optimization tool that maximizes the area utilization while satisfying the social distancing constraints, and also minimizes the overall risk of infection among facilities.

We have proposed a parallel between this problem and that of locating wind turbines in an offshore area, which allowed us to apply state-of-the-art solution approaches for the latter problem to produce optimized facility layouts. We have analyzed alternative definitions of the interference function used to model virus spread (which is just an input in our model) and have compared them on test cases. Then we have addressed possible applications of our optimization methodology, showing that improved solutions can be obtained with less regular (but more efficient) layout patterns than those typically found manually. We have also shown the versatility of our method, by extending it to a family-group seat selection problem arising, e.g., in theaters or airplanes.

Another challenging research direction is the definition of an interference function that models virus spread along specific directions (rather than uniformly over the surrounding space), e.g., because of the presence of air conditioning and/or Plexiglas settings. This would produce very irregular interference matrices (akin to those arising in offshore wind farms with predominant wind scenarios) that are very difficult to handle by a manual solution approach, thus making our methodology even more appealing.

As to models limitations, we believe that explaining the results to a nontechnical audience could be problematic, since the optimized patterns are often counter-intuitive and may look inefficient/unfair at first glance.

Another model limitation comes from the assumption that the overall risk of infection can be measured by adding pairwise contributions (i.e., the entries of an interference matrix), thus excluding more complex situations where the total risk is a nonlinear function of the layout as a whole.

Finally, we want to stress once again that our work does not (and, actually, cannot) give an answer to the delicate problem of deciding which deterministic functional form of the interference is best to describe the transmission of the virus—a topic to be addressed by the community of virologists and epidemiologists. Indeed, the interference function is just an input data for our model, whose definition is delegated to the decision maker.

Acknowledgements

The work of the second author was partially supported by MiUR, Italy (PRIN project). We thank Double-Click SRL, Padua (Italy) for the use of their wind-farm optimization software, and Det Andre Teatret (www.detandreteatret.no) and SINTEF (www.sintef.no/en) for providing us with the theater application. We also

thanks four anonymous referees for their constructive comments leading to an improved presentation of our results.

References

Archer, R., Nates, G., Donovan, S., & Waterer, H. (2011). Wind turbine interference in a wind farm layout optimization – mixed integer linear programming model. *Wind Engineering, 35*(2), 165–178.

Contardo, C. (2020). Decremental clustering for the solution of p-dispersion problems to proven optimality. *INFORMS Journal on Optimization, 2*(2), 134–144.

Fagerfjall, P. (2010). Optimizing Wind Farm Layout - More Bang for the Buck Using Mixed Integer Linear Programming. Master's thesis.Göteborg, Sweden Department of Mathematical Sciences, Chalmers University of Technology and Gothenburg University.

Fischetti, M. (2018). *Mathematical Programming Models and Algorithms for Offshore Wind Park Design*. Technical University of Denmark, DTU Management Ph.D. thesis..

Fischetti, M. (2019). Improving profitability of wind farms with operational research. *Impact, 2019*(1), 30–34.

Fischetti, M. (2021). On the optimized design of next-generation wind farms. *European Journal of Operational Research, 291*(3), 862–870.

Fischetti, M., & Fischetti, M. (2018). Matheuristics. In R. Martí, P. M. Pardalos, & M. G. C. Resende (Eds.), *Handbook of heuristics* (pp. 121–153). Cham: Springer International Publishing.

Fischetti, M., Fischetti, M., & Stoustrup, J. (2020a). Mathematical optimization for social distancing (pre-print), 10.13140/RG.2.2.35799.91049

Fischetti, M., & Fraccaro, M. (2019). Machine learning meets mathematical optimization to predict the optimal production of offshore wind parks. *Computers & Operations Research, 106*, 289–297.

Fischetti, M., Kristoffersen, J. R., Hjort, T., Monaci, M., & Pisinger, D. (2020b). Vattenfall optimizes offshore wind farm design. *INFORMS Journal On Applied Analytics, 50*(1), 80–94.

Fischetti, M., & Monaci, M. (2014). Proximity search for 0–1 mixed-integer convex programming. *Journal of Heuristics, 20*, 709–731.

Fischetti, M., & Monaci, M. (2016). Proximity search heuristics for wind farm optimal layout. *Journal of Heuristics, 22*(4), 459–474.

Fischetti, M., & Pisinger, D. (2019). Mathematical optimization and algorithms for offshore wind farm design: An overview. *Business & Information Systems Engineering, 61*(4), 469–485.

Jensen, N. (1983). A Note on Wind Generator Interaction. *Technical Report Riso-M-2411(EN)*. Riso National Laboratory, Roskilde, Denmark.

Jones, B., Sharpe, P., Iddon, C., Hathway, E. A., Noakes, C. J., & Fitzgerald, S. (2021). Modelling uncertainty in the relative risk of exposure to the SARS-CoV-2 virus by airborne aerosol transmission in well mixed indoor air. *Building and Environment, 191*, 107617.

Kudela, J. (2020). Social distancing as p-dispersion problem. *IEEE Access, 8*, 149402–149411.

Mittal, R., Meneveau, C., & Wu, W. (2020). A mathematical framework for estimating risk of airborne transmission of COVID-19 with application to face mask use and social distancing. *Physics of Fluids, 32*(10), 101903.

Moon, I. D. (1984). An analysis of network location problems with distance constraints. *Management Science, 30*(3), 290307.

Moore, J. F., Carvalho, A., Davis, G. A., Abulhassan, Y., & Megahed, F. M. (2021). Seat assignments with physical distancing in single-destination public transit settings. *IEEE Access, 9*, 42985–42993.

Morawska, L., Tang, J. W., Bahnfleth, W., Bluyssen, P. M., Boerstra, A., Buonanno, G., et al., (2020). How can airborne transmission of COVID-19 indoors be minimised? *Environment International, 142*, 105832.

Noakes, C. J., Beggs, C. B., Sleigh, P. A., & Kerr, K. G. (2006). Modelling the transmission of airborne infections in enclosed spaces. *Epidemiology and Infection, 134*(5), 10821091.

Odgaard, P. F., & Stoustrup, J. (2013). Fault tolerant wind farm control - a benchmark model. In *Proceedings of the 2013 ieee multi-conference on systems and control, Hyderabad, India* (pp. 412–417).

Pavlik, J. A., Ludden, I. G., Jacobson, S. H., & Sewell, E. C. (2021). Airplane seating assignment problem. *Service Science, 13*(1), 1–18.

Prather, K. A., Marr, L. C., Schooley, R. T., McDiarmid, M. A., Wilson, M. E., & Milton, D. K. (2020). Airborne transmission of SARS-CoV-2. *Science, 370*(6514), 303–304. https://doi.org/10.1126/science.abf0521.

Salari, M., Milne, R. J., Delcea, C., Kattan, L., & Cotfas, L.-A. (2020). Social distancing in airplane seat assignments. *Journal of Air Transport Management, 89*, 101915.

Samet, J. M., Prather, K., Benjamin, G., Lakdawala, S., Lowe, J.-M., Reingold, A., et al., (2021). Airborne transmission of severe acute respiratory syndrome coronavirus 2 (SARS-CoV-2): What we know. *Clinical Infectious Diseases*. https://doi.org/10.1093/cid/ciab039.

Sayah, D., & Irnich, S. (2017). A new compact formulation for the discrete p-dispersion problem. *European Journal of Operational Research, 256*(1), 62–67.

Tang, J., Bahnfleth, W., Bluyssen, P., Buonanno, G., Jimenez, J., Kurnitski, J., et al., (2021). Dismantling myths on the airborne transmission of severe acute respiratory syndrome coronavirus-2 (SARS-CoV-2). *Journal of Hospital Infection, 110*, 89–96.

Ugail, H., Aggarwal, R., Iglesias, A., Howard, N., Campuzano, A., Suárez, P., et al., (2021). Social distancing enhanced automated optimal design of physical spaces in the wake of the COVID-19 pandemic. *Sustainable Cities and Society, 68*, 102791.

Zhao, T., Cheng, C., Liu, H., & Sun, C. (2020). Is one- or two-meters social distancing enough for COVID-19? Evidence for reassessing. *Public Health, 185*, 87. https://doi.org/10.1016/j.puhe.2020.06.005.